COMMUNICATION

A Polythiophene Derivative with Superior Properties for Practical Application in Polymer Solar Cells

Maojie Zhang, Xia Guo, Wei Ma,* Harald Ade, and Jianhui Hou*

Polymer solar cells (PSCs) have attracted much attention in recent years because of their advantages of low cost, easy fabrication, light weight, and the possibility of using them to fabricate flexible large-area devices.[1–3] In the past decade, a great many conjugated polymers have been designed, synthesized, and applied as donor materials in PSCs. Among these polymers, polythiophene (PT) derivatives[4–9] are one of the most important types of donor materials, the most prominent of which is regioregular poly(3-hexylthiophene) (P3HT), which is also a classic photovoltaic donor material. As is well known, P3HT has played a very important role in advancing the development of the field of PSCs. Under optimal device fabrication conditions, the PSCs based on P3HT:[6, 6]-phenyl C_{71} butyric acid methyl ester (P3HT:PC$_{71}$BM) and P3HT:indene-C_{70} bisadduct (P3HT:IC$_{70}$BA) typically show power conversion efficiencies (PCEs) of ca. 4%[4] and ca. 7%,[5b] respectively, and these results are among the highest values in the field.

Much effort has been devoted to designing PT derivatives to realize higher efficiency in PSCs, that is, to exploring PT derivatives with better photovoltaic properties than P3HT. For example, the PT derivatives with two-dimensional (2D) conjugated structure showed enhanced light absorption properties compared to P3HT;[6a] the PT derivative P3HDTTT (shown in **Figure 1**) with fewer electron-donating groups showed a lower highest occupied molecular orbit (HOMO) level and thus higher open circuit voltage (V_{oc}) than P3HT in PSCs.[6b] More recently, a series of PT derivatives (named PT-C1, PT-C2, and PT-C3) containing carboxylate substituents were reported and the PSCs based on PT-C3 (Figure 1) showed improved V_{oc} of 0.78 V in comparison with the P3HT-based PSCs.[7] Besides the polymers mentioned above, there are many interesting examples of molecular structure optimization of PT derivatives.[8–13] Hence, it is attractive to improve the photovoltaic performance of PT derivatives by molecular structure modification.

In the work reported here, a new PT derivative, poly[5,5′-bis(2-butyloctyl)-(2,2′-bithiophene)-4,4′-dicarboxylate-alt-5,5′-2,2′-bithiophene] (PDCBT, shown in **Scheme 1**), was

designed and synthesized. By attaching electron-withdrawing carboxylate substituents to the side chain, it is possible to reduce the HOMO level from –4.90 eV for P3HT to –5.26 eV for PDCBT with minor effect on the optical bandgap. PDCBT is highly crystalline and exhibits compact π–π stacking with a smaller separation than P3HT. The PSCs based on PDCBT/PC$_{71}$BM (1:1, w/w) fabricated under optimal conditions exhibit a PCE of 7.2% with V_{oc} = 0.91 V, short-circuit current density J_{sc} = 11.0 mA cm^{-2}, and fill factor FF = 72.0%. In contrast, the PSCs based on P3HT/PC$_{71}$BM (1:1, w/w) fabricated under the same conditions showed a PCE of only 1.8% with V_{oc} = 0.63 V, J_{sc} = 4.5 mA cm^{-2}, and FF = 62%. Furthermore, the performance of PSCs based on PDCBT is insensitive to variations of active layer thickness and processing conditions such as additives and thermal treatment. In addition, compared with other high-efficiency low-bandgap photovoltaic materials,[13–15] this polymer exhibits a simpler structure and easier synthesis, which is beneficial for mass production. These results indicate that PDCBT has great potential in large-scale manufacturing of low-cost, high-performance PSCs and also will be a more suitable candidate than P3HT as the broad-bandgap material in tandem solar cells.

As shown in Scheme 1, the polymer PDCBT can be prepared by four steps, starting from commercially available chemicals, and it shows good solubility in common solvents such as chloroform (CF), chlorobenzene (CB), *ortho*-dichlorobenzene (*o*-DCB), and so on. Since the backbone of the polymer consists of thiophene units and the functional groups used to modulate its properties are carboxylates only, this polymer can be easily synthesized and also the synthetic method has great potential for optimization.

The absorption spectra of PDCBT and P3HT in solid films are shown in **Figure 2**a. In comparison with P3HT, PDCBT shows a similar absorption edge located at 650 nm, corresponding to a bandgap (E_g^{opt}) of 1.9 eV. However, the main absorption peak of PDCBT is located at 551 nm, which is

Dr. M. J. Zhang, X. Guo, Prof. J. H. Hou
State Key Laboratory of Polymer
Physics and Chemistry
Institute of Chemistry
Chinese Academy of Sciences
Beijing 100190, P. R. China
E-mail: hjhzlz@iccas.ac.cn
Dr. W. Ma, Prof. H. Ade
Department of Physics
North Carolina State University
Raleigh, NC 27695, USA
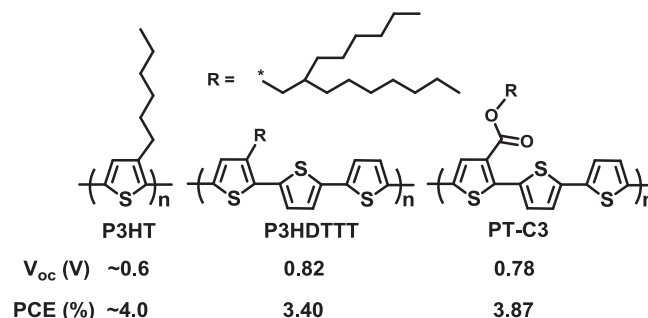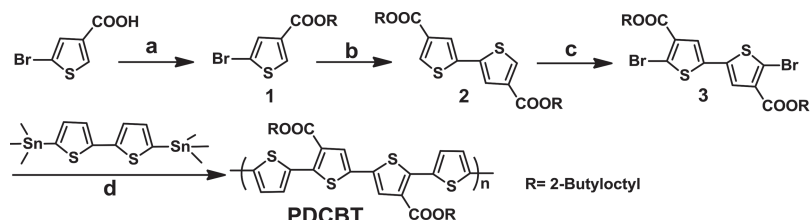E-mail: wma5@ncsu.edu

	P3HT	P3HDTTT	PT-C3
V_{oc} (V)	~0.6	0.82	0.78
PCE (%)	~4.0	3.40	3.87

Figure 1. Molecular structures and basic photovoltaic properties of P3HT and two PT derivatives with different side groups.

Materials
Views
www.MaterialsViews.com

ADVANCED
MATERIALS
www.advmat.de

Scheme 1. Synthetic routes and molecular structure of PDCBT. Reagents and conditions: a) DCC (N,N'-dicyclohexylcarbodiimide), DMAP (4-dimethylaminopyridine), 2-butyloctan-1-ol, yield: 85%; b) KI, Zn, PPh$_3$ (triphenylphosphine), Ni(PPh$_3$)$_2$Cl$_2$, 50 °C, yield: 70%; c) CF$_3$COOH/CHCl$_3$, NBS (N-bromosuccinimide), yield: 60%; d) toluene, Pd(PPh$_3$)$_4$, 110 °C, yield: 76%.

37 nm red-shifted compared to that of P3HT. Interestingly, the absorption coefficient of the PDCBT film is 1.05×10^5 cm^{-1}, which is ca. 30% higher than that of P3HT film, implying that PDCBT film can utilize sunlight more efficiently than P3HT film of the same thickness.

Electrochemical cyclic voltammetry (CV) was performed to determine the HOMO and the lowest unoccupied molecular

orbital (LUMO) levels of the conjugated polymers.[16] Figure 2b shows the CV plots of PDCBT and P3HT films on a platinum electrode in 0.1 mol L^{-1} Bu$_4$NPF$_6$ acetonitrile solution, respectively. The onset oxidation potentials (φ_{ox}) are 0.19 and 0.55 V versus Ag/Ag$^+$. From φ_{ox} of the polymers, HOMO levels of the polymers, in electron volts, were calculated according to the equation[17] HOMO = $-e$ (φ_{ox} + 4.71). The HOMO levels of PDCBT and P3HT are −4.90 and −5.26 eV, respectively. It is very clear that attaching the electron-withdrawing carboxylate substituent to the side chains made the HOMO level of PDCBT decrease by 0.36 eV in comparison with P3HT, which is beneficial for achieving higher V_{oc} in PSCs.

PSC devices were fabricated and characterized to investigate the photovoltaic properties of the polymer. The device structure used in this work was ITO/PEDOT:PSS (30 nm)/polymer:PC$_{71}$BM/Ca (20 nm)/Al (80 nm), where ITO is indium tin oxide, PEDOT is poly(3,4-ethylenedioxythiophene), and PSS is poly(styrene sulfonate). Initially, PSC devices with different donor/acceptor (D/A) ratios (PDCBT/PC$_{71}$BM, w/w) were fabricated. **Figure 3**a shows the current density–voltage (J–V) curves of the devices under AM 1.5G, that is, standard solar spectrum (100 mW cm^{-2}) illumination with different D/A ratios (1.5:1, 1:1, and 1:1.5); the corresponding photovoltaic parameters are summarized in **Table 1**. It is clear that the optimal D/A ratio of the blend is 1:1, and a PCE of 6.9% was obtained with V_{oc} = 0.94 V, J_{sc} = 10.2 mA cm^{-2}, and FF = 72%. Under the same conditions, the device based on P3HT/PC$_{71}$BM (1:1, w/w) exhibited a PCE of only 1.8% with V_{oc} = 0.63 V, J_{sc} = 4.5 mA cm^{-2}, and FF = 62%; under optimal conditions, that is, using the solvent annealing method and with an active layer thickness of 210 nm, the device based on P3HT/PC$_{71}$BM (1:1, w/w) exhibited a PCE of 3.9% with V_{oc} = 0.59 V, J_{sc} = 9.6 mA cm^{-2}, and FF = 69%. In order to further investigate the advantages of PDCBT compared to P3HT, we fabricated PSCs based on P3HT or PDCBT/PC$_{61}$BM under the optimal conditions shown in Figure S1 (Supporting Information) and Table 1. The PSCs based on PDCBT/PC$_{61}$BM (1:1, w/w) exhibited a PCE of 6.3% with V_{oc} = 0.90 V, J_{sc} = 11.1 mA cm^{-2}, and FF = 63%. In contrast, the PSCs based on P3HT/PC$_{61}$BM (1:1, w/w) showed a PCE of 3.9% with V_{oc} = 0.61 V, J_{sc} = 9.7 mA cm^{-2}, and FF = 65%. In addition, the photovoltaic performance of the PSCs based on P3HT or PDCBT/PC$_{61}$BM under other conditions was also explored, as shown in Figure S1 and Table S1 in the Supporting Information. It is clear that the PDCBT/PC$_{61}$BM-based PSCs exhibit better photovoltaic performance than the P3HT/PC$_{61}$BM-based PSCs under various conditions.

The external quantum efficiency (EQE) spectra of the PDCBT-based device and the P3HT-based device fabricated under the optimal conditions are shown in Figure 3b. The device based on PDCBT/PC$_{71}$BM (1:1, w/w) exhibits a response range from 350 nm to 650 nm, with a maximum EQE value of 75% at 470 nm. Compared with the P3HT-based device, the PDCBT-based device shows a significant improvement of EQE in the wavelength range 450–600 nm, which means more efficient photoelectron conversion in this range and hence
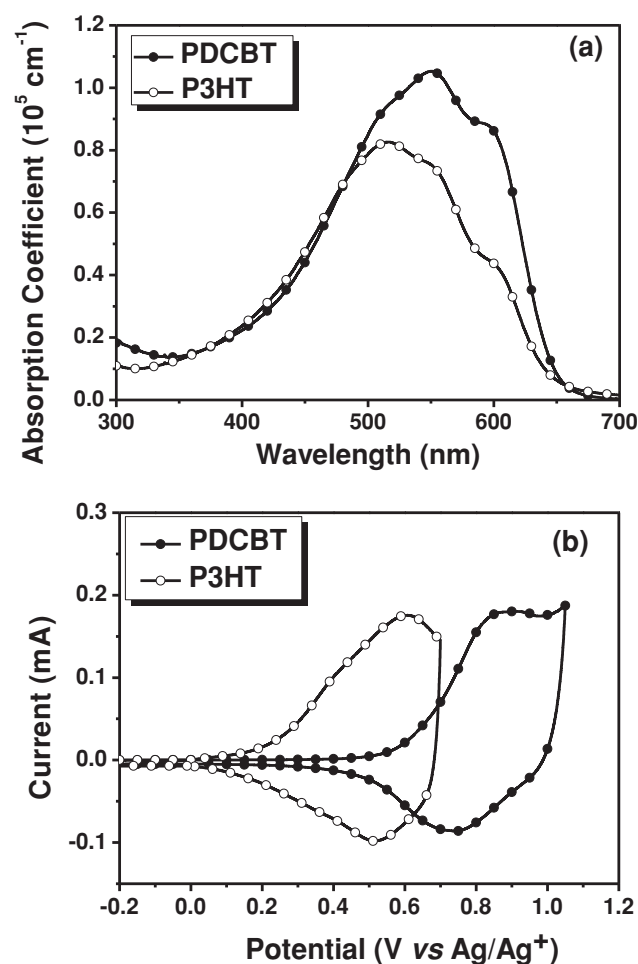

Figure 2. a) The absorption spectra of PDCBT and P3HT films. b) Cyclic voltammograms of PDCBT film and P3HT film on a platinum electrode measured in 0.1 mol L^{-1} Bu$_4$NPF$_6$ acetonitrile solutions at a scan rate of 50 mV s^{-1}.
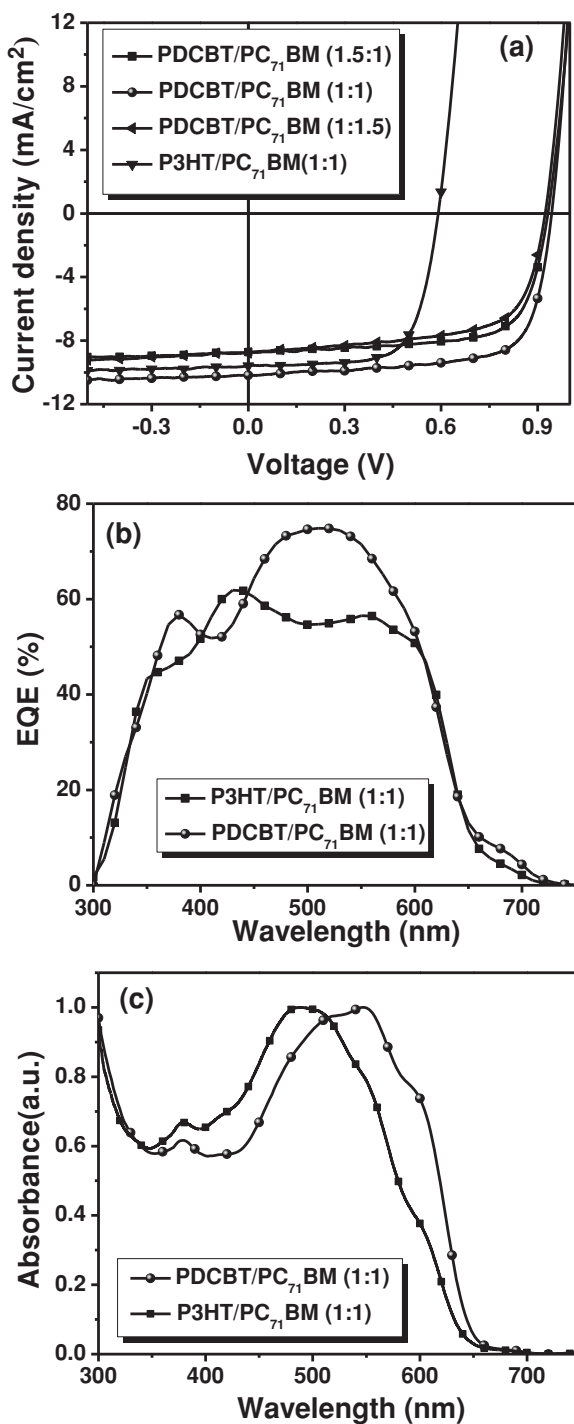
Figure 3. a) The *J*–*V* curves of PSCs based on PDCBT or P3HT. b) EQE curves of PSCs based on PDCBT or P3HT/PC$_{71}$BM (1:1, w/w). c) The normalized absorption of the blend film of PDCBT or P3HT/PC$_{71}$BM (1:1, w/w).

Table 1. Photovoltaic performances of the PSCs under AM 1.5G illumination, 100 mW cm^{-2}.

Active layers	D/A [w/w]	Thickness [nm]	V_{oc} [V]	J_{sc} [mA cm^{-2}]	FF [%]	$PCE_{max}(PCE_{ave}$[f]$)$ [%]
PDCBT/ PC$_{71}$BM	1.5:1	95	0.93	8.8	71	5.8 (5.6)
	1:1	70	0.93	9.9	71	6.5 (6.3)
	1:1	95	0.94	10.2	72	6.9 (6.7)
	1:1[a]	94	0.91	11.0	72	7.2 (7.0)
	1:1[b]	95	0.95	10.5	69	6.9 (6.7)
	1:1	110	0.92	10.3	70	6.6 (6.3)
	1:1	150	0.92	10.5	68	6.5 (6.2)
	1:1	230	0.91	10.6	66	6.4 (6.1)
	1:1.5	95	0.92	8.8	66	5.3 (5.2)
PDCBT/ PC$_{61}$BM	1:1	95	0.90	11.1	63	6.3 (6.1)
P3HT/ PC$_{71}$BM	1:1[c]	90	0.63	4.5	62	1.8 (1.7)
	1:1[d]	210	0.59	9.6	69	3.9 (3.8)
P3HT/ PC$_{61}$BM	1:1[e]	220	0.61	9.7	65	3.9 (3.7)

[a] With 3% DIO; [b] With thermal annealing at 100 °C for 10 min; [c] The devices were fabricated under the same conditions as used for PDCBT/PC$_{71}$BM-based devices; [d] The devices were fabricated with solvent annealing; [e] The devices were fabricated under the optimal conditions from the literature;[4a] [f] The average PCE was obtained from over 20 devices.

P3HT/PC$_{71}$BM blend. The enhancement of absorbance at long wavelengths will contribute to the improvement of J_{sc}.

Furthermore, in order to study the relationship between the photovoltaic performance of the PDCBT-based PSCs and the device fabrication conditions, the following investigations were carried out. First, the widely used solvent additive 1,8-diiodooctane (DIO) was used to further improve photovoltaic performance of the devices. As shown in **Figure 4**a and Table 1, when 3% DIO was used as a solvent additive, the PCE of the PDCBT-based device was improved to 7.2%, which is slightly higher than the device processed using pure *o*-DCB. Then the effect of thermal annealing on photovoltaic performance was also investigated. Because the glass transition temperature of poly(ethylene terephthalate) (PET), the transparent substrate material that is widely used for making flexible PSCs, is ca. 80°, the blend film of PDCBT/PC$_{71}$BM was treated under 100 °C for 10 min. As shown in Figure 4a and Table 1, after the thermal annealing process, there is no change in photovoltaic properties, meaning that the blend of PDCBT/PC$_{71}$BM is robust enough to endure the thermal treatment process for making flexible devices. Finally, we also investigated the relationship between the thickness of the active layers and the photovoltaic performance. As shown in Figure 4a and Table 1, benefiting from the strong absorption coefficient, the PDCBT-based PSC with 70 nm thick active layer still exhibited a high J_{sc} of 9.9 mA cm^{-2}. Interestingly, when the thickness increased from 70 nm to 230 nm gradually, the *FF* values of the devices dropped slightly from over 70% to ca. 66%, while the J_{sc} and V_{oc} values of the devices remained virtually unchanged. As a
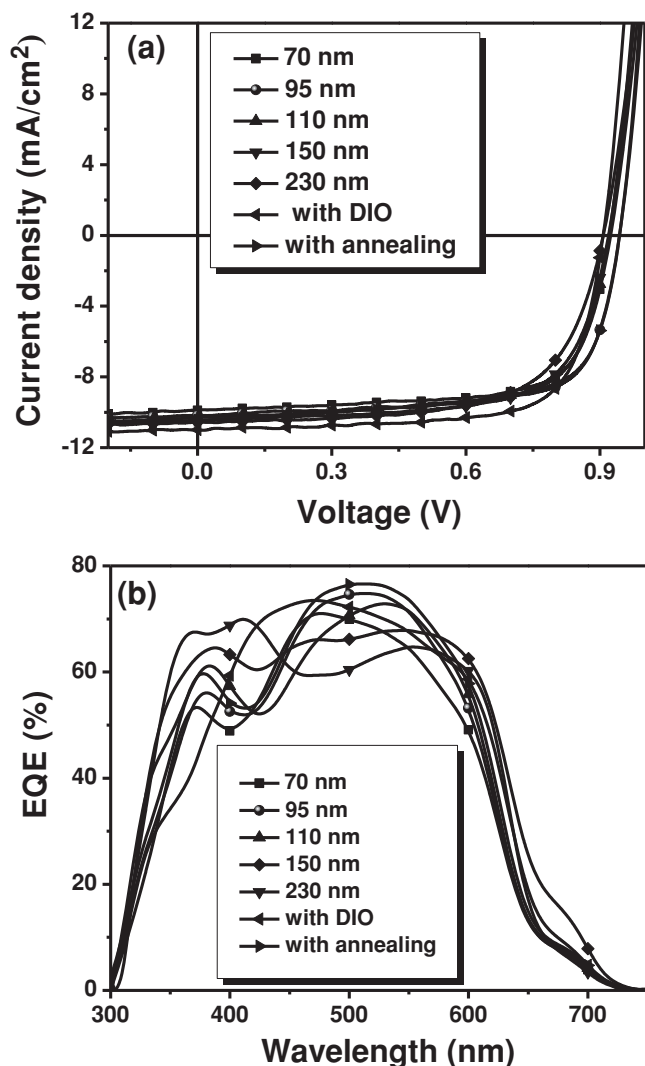
benefits for the improvement of J_{sc}. The variations between the integral values deduced from the EQE curves and the standard solar spectrum (AM 1.5G) and the measured values are below 5%. Furthermore, as shown in Figure 3c, the blend of PDCBT/PC$_{71}$BM (1:1, w/w) exhibits stronger absorption in the long-wavelength range 510–650 nm compared with that of the

Materials
Views
www.MaterialsViews.com

ADVANCED
MATERIALS
www.advmat.de

COMMUNICATION

Figure 4. The *J–V* curves (a) and the corresponding EQE curves (b) of PSCs based on PDCBT/PC$_{71}$BM (1:1, w/w) with different processing conditions.

result, when the active layer thickness changed from 70 nm to 230 nm, the variation of PCE was (6.6 ± 0.3)%. According to these above investigations, it can be concluded that the photovoltaic performance of the PDCBT/PC$_{71}$BM-based device is insensitive to the device fabrication conditions.

Grazing incidence X-ray diffraction (GIXD) measurements were carried out to investigate molecular packing of the neat PDCBT film and the blend film of PDCBT and PC$_{71}$BM. **Figure 5**a shows 2D GIXD images and the in-plane (IP) and out-of-plane (OOP) GIXD profiles of the samples, including thin films for pure PDCBT and the PDCBT/PC$_{71}$BM (1:1, w/w) blend film cast from pure *o*-DCB. The OOP profile of the pure polymer film showed pronounced 100, 200, and 300 diffraction peaks at 0.31 Å^{-1}, 0.62 Å^{-1} and 0.93 Å^{-1}, respectively, arising from the alkyl chain packing with *d*-spacing of ca. 20 Å. This indicates a highly crystallized nature of the PDCBT. Impressively, in the IP profile, it showed one sharp and intensive peak at ca. 1.7 Å^{-1}, which corresponds to (010) π–π stacking with the *d*-spacing of 3.7 Å. This suggests an edge-on dominated molecular orientation with respect to the substrate. Moreover, on going from the pure polymer film to the blend film, the crystalline structure of the polymer is well maintained. Compared with that of P3HT, PDCBT exhibited smaller π–π stacking spacing in the neat film, which means more compact inter-chain packing and benefits for π-electron hopping among the polymer chains.[18]

The bulk morphology of the blend of PDCBT and PC$_{71}$BM was investigated by resonant soft X-ray scattering (RSoXS).[19] X-rays with photon energy of 283 eV were utilized to enhance the contrast between PDCBT and PC$_{71}$BM and also to minimize the fluorescence background. The measurements were performed in transmission geometry with the diffraction vector being in the plane of the film. Figure 5b shows the RSoXS profiles for PDCBT/PC$_{71}$BM (1:1, w/w) blends cast from *o*-DCB. As shown in Figure 5b, the median s_{median} of the spatial frequency distribution $s = q/2\pi$ corresponds to the characteristic median length scale, ξ, of the corresponding log-normal distribution in real space, with $\xi = 1/s_{median}$ a model-independent statistical quantity. The ξ of the blend showed a multi-modal distribution that can be fitted very well with two log-normal distributions, that
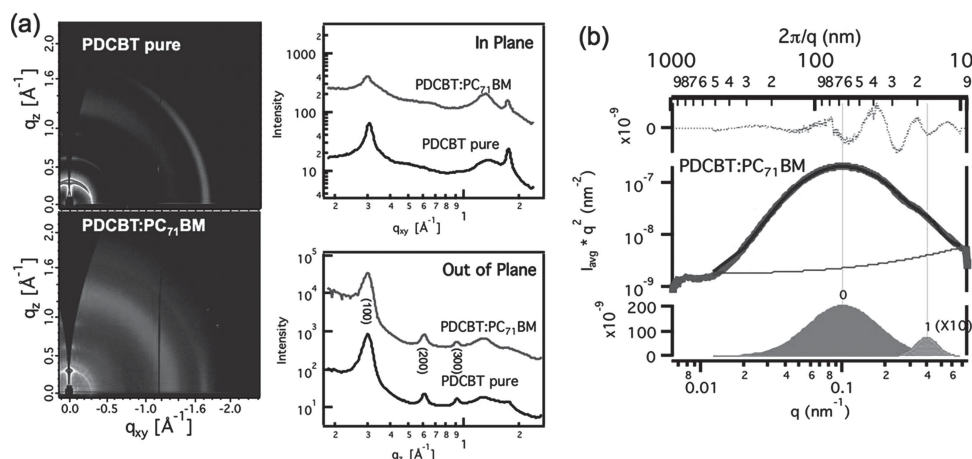

Figure 5. a) Two-dimensional GIXD images and integrated scattering of neat PDCBT film and PDCBT/PC$_{71}$BM blend films. b) RSoXS profiles for PDCBT/PC$_{71}$BM (1:1, w/w) blend.

is, two well-defined peaks with ξ of ca. 20 nm and ca. 50 nm. Such multiple-length-scale phase separation is observed in other blends too and is considered to be favorable for charge separation and transport.[20] Furthermore, atomic force microscopy (AFM) and transmission electron microscopy (TEM) methods were used to give complementary, real-space morphological information about the PDCBT/PC$_{71}$BM (1:1, w/w) blend film (see Figure S2 in the Supporting Information). As shown in Figure S2a, the root-mean-square (RMS) value of the blend film is 0.86 nm, obtained by AFM. In the TEM images (see Figure S2b), dark and light domains can be clearly distinguished, indicating that a network of the polymer and PC$_{71}$BM is formed. These results are consistent with the RSoXS results.

In conclusion, a PT derivative with simple molecular structure, PDCBT, was easily synthesized for photovoltaic applications. PDCBT showed a lower HOMO level (−5.26 eV) and better light-harvesting ability (maximum absorption coefficient 1.05×10^5 cm^{-1}) than P3HT. The best device based on PDCBT/PC$_{71}$BM (1:1,w/w) exhibited a good PCE of 7.2% with a high V_{oc} of 0.91 V and a high FF of 72%. The EQE of the device reached 75% so that a J_{sc} of 11 mA cm^{-2} was obtained, which is a high value for a polymer with a bandgap of 1.9 eV. Furthermore, the device performance is not sensitive to variation of the device processing conditions, such as addition of solvent additives (e.g., DIO) and thermal treatment. In addition, when the active layer thickness was changed from 70 nm to 230 nm, the photovoltaic performance of the PDCBT-based device changed little.

The PCE of 7.2% is an outstanding result for the polymers with absorption edge at 650 nm. Thus, PDCBT is a promising candidate material to take over the role of P3HT in PSCs with single and tandem structures. More importantly, this work suggests that the design of new polymers with superior properties for practical applications should also be considered, which will definitely benefit the industrialization of PSC technology.

Supporting Information

Supporting Information is available from the Wiley Online Library or from the author.

Acknowledgements

[1] a) J. W. Chen, Y. Cao, *Acc. Chem. Res.* **2009**, *42*, 1709–1718; b) Y. F. Li, *Acc. Chem. Res.* **2012**, *45*, 723–733; c) I. McCulloch, R. S. Ashraf, L. Biniek, H. Bronstein, C. Combe, J. E. Donaghey, D. I. James, C. B. Nielsen, B. C. Schroeder, W. M. Zhang, *Acc. Chem. Res.* **2012**, *45*, 714–722.

[2] a) C. J. Brabec, S. Gowrisanker, J. J. M. Halls, D. Laird, S. J. Jia, S. P. Williams, *Adv. Mater.* **2010**, *22*, 3839–3856; b) G. Dennler, M. C. Scharber, C. J. Brabec, *Adv. Mater.* **2009**, *21*, 1323–1338; c) B. C. Thompson, J. M. J. Fréchet, *Angew. Chem. Int. Ed.* **2008**, *47*, 58–77; d) P. M. Beaujuge, J. M. J. Fréchet, *J. Am. Chem. Soc.* **2011**, *133*, 20009–20029.

[3] a) Z. B. Henson, K. Müllen, G. C. Bazan, *Nat. Chem.* **2012**, *4*, 699–704; b) G. Li, R. Zhu, Y. Yang, *Nat. Photonics* **2012**, *6*, 153–161.

[4] a) W. Ma, C. Yang, X. Gong, K. Lee, A. J. Heeger, *Adv. Funct. Mater.* **2005**, *15*, 1617–1622; b) M. T. Dang, L. Hirsch, G. Wantz, J. D. Wuest, *Chem. Rev.* **2013**, *113*, 3734–3765; c) Y. Kim, S. Cook, S. M. Tuladhar, S. A. Choulis, J. Nelson, J. R. Durrant, D. D. Bradley, M. Giles, I. McCulloch, C.-S. Ha, *Nat. Mater.* **2006**, *5*, 197–203; d) G. Li, V. Shrotriya, J. Huang, Y. Yao, T. Moriarty, K. Emery, Y. Yang, *Nat. Mater.* **2005**, *4*, 864–868.

[5] a) Y. J. He, H. Y. Chen, J. H. Hou, Y. F. Li, *J. Am. Chem. Soc.* **2010**, *132*, 1377–1382; b) X. Guo, C. Cui, M. Zhang, L. Huo, Y. Huang, J. Hou, Y. Li, *Energy Environ. Sci.* **2012**, *5*, 7943–7949; c) G. J. Zhao, Y. J. He, Y. F. Li, *Adv. Mater.* **2010**, *22*, 4355–4358.

[6] a) J. H. Hou, Z. A. Tan, Y. Yan, Y. J. He, C. H. Yang, Y. F. Li, *J. Am. Chem. Soc.* **2006**, *128*, 4911–4916; b) J. Hou, T. L. Chen, S. Zhang, L. Huo, S. Sista, Y. Yang, *Macromolecules* **2009**, *42*, 9217–9219.

[7] M. J. Zhang, X. Guo, Y. Yang, J. Zhang, Z. G. Zhang, Y. F. Li, *Polym. Chem.* **2011**, *2*, 2900–2906.

[8] a) S. Gunes, H. Neugebauer, N. S. Sariciftci, *Chem. Rev.* **2007**, *107*, 1324–1338; b) Y. J. Cheng, S. H. Yang, C. S. Hsu, *Chem. Rev.* **2009**, *109*, 5868–5923; c) P. L. T. Boudreault, A. Najari, M. Leclerc, *Chem. Mater.* **2011**, *23*, 456–469; d) C. L. Chochos, S. A. Choulis, *Prog. Polym. Sci.* **2011**, *36*, 1326–1414.

[9] a) E. J. Zhou, Z. Tan, Y. Yang, L. J. Huo, Y. P. Zou, C. H. Yang, Y. F. Li, *Macromolecules* **2007**, *40*, 1831–1837; b) Z. G. Zhang, S. Zhang, J. Min, C. Cui, H. Geng, Z. Shuai, Y. Li, *Macromolecules* **2012**, *45*, 2312–2320; c) C. Cui, Y. Sun, Z. G. Zhang, M. Zhang, J. Zhang, Y. Li, *Macromol. Chem. Phys.* **2012**, *213*, 2267–2274; d) H. Bronstein, M. Hurhangee, E. C. Fregoso, D. Beatrup, Y. W. Soon, Z. Huang, A. Hadipour, P. S. Tuladhar, S. Rossbauer, E.-H. Sohn, *Chem. Mater.* **2013**, *25*, 4239–4249; e) C.-H. Cho, H. J. Kim, H. Kang, T. J. Shin, B. J. Kim, *J. Mater. Chem.* **2012**, *22*, 14236–14245; f) X. Guo, M. J. Zhang, L. J. Huo, C. H. Cui, Y. Wu, J. H. Hou, Y. F. Li, *Macromolecules* **2012**, *45*, 6930–6937.

[10] a) L. M. Kozycz, D. Gao, J. Hollinger, D. S. Seferos, *Macromolecules* **2012**, *45*, 5823–5832; b) S. Ko, E. T. Hoke, L. Pandey, S. Hong, R. Mondal, C. Risko, Y. Yi, R. Noriega, M. D. McGehee, J.-L. Brédas, A. Salleo, Z. Bao, *J. Am. Chem. Soc.* **2012**, *134*, 5222–5232; c) C.-Y. Yu, B.-T. Ko, C. Ting, C.-P. Chen, *Sol. Energy Mater. Sol. Cells* **2009**, *93*, 613–620; d) C. Lu, H. C. Wu, Y. C. Chiu, W. Y. Lee, W. C. Chen, *Macromolecules* **2012**, *45*, 3047–3056.

[11] a) H. Xin, F. S. Kim, S. A. Jenekhe, *J. Am. Chem. Soc.* **2008**, *130*, 5424–5425; b) H. Xin, G. Q. Ren, F. S. Kim, S. A. Jenekhe, *Chem. Mater.* **2008**, *20*, 6199–6207; c) P. T. Wu, H. Xin, F. S. Kim, G. Q. Ren, S. A. Jenekhe, *Macromolecules* **2009**, *42*, 8817–8826; d) G. Ren, P.-T. Wu, S. A. Jenekhe, *Chem. Mater.* **2010**, *22*, 2020–2026.

[12] a) K. Sivula, C. K. Luscombe, B. C. Thompson, J. M. J. Fréchet, *J. Am. Chem. Soc.* **2006**, *128*, 13988–13989; b) S. Miyanishi, K. Tajima, K. Hashimoto, *Macromolecules* **2009**, *42*, 1610–1618; c) J. S. Kim, Y. Lee, J. H. Lee, J. H. Park, J. K. Kim, K. Cho, *Adv. Mater.* **2010**, *22*, 1355–1360; d) Y. T. Chang, S. L. Hsu, M. H. Su, K. H. Wei, *Adv. Mater.* **2009**, *21*, 2093–2097.

Materials
Views
www.MaterialsViews.com

ADVANCED
MATERIALS
www.advmat.de

COMMUNICATION

[13] a) S. H. Park, A. Roy, S. Beaupré, S. Cho, N. Coates, J. S. Moon, D. Moses, M. Leclerc, K. Lee, A. J. Heeger, *Nat. Photonics* **2009**, *3*, 297–302; b) P. M. Beaujuge, W. Pisula, H. N. Tsao, S. Ellinger, K. Müllen, J. R. Reynolds, *J. Am. Chem. Soc.* **2009**, *131*, 7514–7515; c) X. Guo, M. J. Zhang, J. H. Tan, S. Q. Zhang, L. J. Huo, W. P. Hu, Y. F. Li, J. H. Hou, *Adv. Mater.* **2012**, *24*, 6536–6541; d) Y. X. Xu, C. C. Chueh, H. L. Yip, F. Z. Ding, Y. X. Li, C. Z. Li, X. S. Li, W. C. Chen, A. K. Y. Jen, *Adv. Mater.* **2012**, *24*, 6356–6361; e) K. H. Hendriks, G. H. L. Heintges, V. S. Gevaerts, M. M. Wienk, R. A. J. Janssen, *Angew. Chem. Int. Ed.* **2013**, *52*, 8341–8344.

[14] Y. Y. Liang, Z. Xu, J. B. Xia, S. T. Tsai, Y. Wu, G. Li, C. Ray, L. P. Yu, *Adv. Mater.* **2010**, *22*, E135-E138.

[15] L. J. Huo, S. Q. Zhang, X. Guo, F. Xu, Y. F. Li, J. H. Hou, *Angew. Chem. Int. Ed.* **2011**, *50*, 9697–9702.

[16] Y. F. Li, Y. Cao, J. Gao, D. L. Wang, G. Yu, A. J. Heeger, *Synth. Met.* **1999**, *99*, 243–248.

[17] Q. J. Sun, H. Q. Wang, C. H. Yang, Y. F. Li, *J. Mater. Chem.* **2003**, *13*, 800–806.

[18] a) X. G. Guo, N. J. Zhou, S. J. Lou, J. W. Hennek, R. P. Ortiz, M. R. Butler, P. L. T. Boudreault, J. Strzalka, P. O. Morin, M. Leclerc, J. T. L. Navarrete, M. A. Ratner, L. X. Chen, R. P. H. Chang, A. Facchetti, T. J. Marks, *J. Am. Chem. Soc.* **2012**, *134*, 18427–18439; b) N. J. Zhou, X. G. Guo, R. P. Ortiz, S. Q. Li, S. M. Zhang, R. P. H. Chang, A. Facchetti, T. J. Marks, *Adv. Mater.* **2012**, *24*, 2242–2248.

[19] a) S. Swaraj, C. Wang, H. P. Yan, B. Watts, L. N. Jan, C. R. McNeill, H. Ade, *Nano Lett.* **2010**, *10*, 2863; b) B. A. Collins, Z. Li, C. R. McNeill, H. Ade, *Macromolecules* **2011**, *44*, 9747–9751; c) Wang, D. H. Lee, A. Hexemer, M. I. Kim, W. Zhao, H. Hasegawa, H. Ade, T. P. Russell, *Nano Lett.* **2011**, *11*, 3906–3911; d) Y. Gu, C. Wang, T. P. Russell, *Adv. Energy Mater.* **2012**, *2*, 683–690; e) F. Liu, Y. Gu, C. Wang, W. Zhao, D. Chen, A. L. Briseno, T. P. Russell, *Adv. Mater.* **2012**, *24*, 3947–3951; f) W. Ma, J. R. Tumbleston, M. Wang, E. Gann, F. Huang, H. Ade, *Adv. Energy Mater.* **2013**, *3*, 864–872.

[20] a) M. J. Zhang, X. Guo, W. Ma, S. Q. Zhang, L. J. Huo, H. Ade, J. H. Hou, *Adv. Mater.* **2014**, *26*, 2089–2095; b) M. J. Zhang, Y. Gu, X. Guo, F. Liu, S. Zhang, L. Huo, T. P. Russell, J. H. Hou, *Adv. Mater.* **2013**, *25*, 4944–4949; c) W. Chen, T. Xu, F. He, W. Wang, C. Wang, J. Strzalka, Y. Liu, J. Wen, D. J. Miller, J. Chen, K. Hong, L. Yu, S. B. Darling, *Nano Lett.* **2011**, *11*, 3707–3713; d) F. Liu, W. Zhao, J. R. Tumbleston, C. Wang, Y. Gu, D. Wang, A. L. Briseno, H. Ade, T. P. Russell, *Adv. Energy Mater.* **2014**, *4*, 1301377; e) M. J. Zhang, X. Guo, S. Q. Zhang, J. H. Hou, *Adv. Mater.* **2014**, *26*, 1118–1123.

[21] A. Hexemer, W. Bras, J. Glossinger, E. Schaible, E. Gann, R. Kirian, A. MacDowell, M. Church, B. Rude, H. Padmore, *J. Phys. Conf. Ser.* **2010**, *247*, 012007.

[22] E. Gann, A. T. Young, B. A. Collins, H. Yan, J. Nasiatka, H. A. Padmore, H. Ade, A. Hexemer, C. Wang, *Rev. Sci. Instrum.* **2012**, *83*, 045110.